TOPICAL REVIEW — Low-dimensional nanostructures and devices

Controllable synthesis of fullerene nano/microcrystals and their structural transformation induced by high pressure*

Yao Ming-Guang(姚明光), Du Ming-Run(杜明润), and Liu Bing-Bing(刘冰冰)†

State Key Laboratory of Superhard Materials, Jilin University, Changchun 130012, *China*

(Received 16 August 2013)

Fullerene molecules are interesting materials because of their unique structures and properties in mechanical, electrical, magnetic, and optical aspects. Current research is focusing on the construction of well-defined fullerene nano/microcrystals that possess desirable structures and morphologies. Further tuning the intermolecular interaction of the fullerene nano/microcrystals by use of pressure is an efficient way to modify their structures and properties, such as creation of nanoscale polymer structures and new hybrid materials, which expands the potential of such nanoscale materials for direct device components. In this paper, we review our recent progress in the construction of fullerene nanostructures and their structural transformation induced by high pressure. Fullerene nano/microcrystals with controllable size, morphology and structure have been synthesized through the self-assembly of fullerene molecules by a solvent-assisted method. By virtue of high pressure, the structures, components, and intermolecular interactions of the assemblied fullerene nano/microcrystals can be finely tuned, thereby modifying the optical and electronic properties of the nanostructures. Several examples on high pressure induced novel structural phase transition in typical fullerene nanocrystals with C_{60} or C_{70} cage serving as building blocks are presented, including high pressure induced amorphization of the nanocrystals and their bulk moduli, high pressure and high temperature (HPHT) induced polymerization in C_{60} nanocrystals, pressure tuned reversible polymerization in ferrocene-doped C_{60}/C_{70} single crystal, as well as unique long-range ordered crystal with amorphous nanoclusters serving as building blocks in solvated C_{60} crystals, which brings new physical insight into the understanding of order and disorder concept and new approaches to the design of superhard carbon materials. The nanosize and morphology effects on the transformations of fullerene nanocrystals have also been discussed. These results provide the foundation for the fabrication of pre-designed and controllable geometries, which is critical in fullerenes and relevant materials for designing nanometer-scale electronic, optical, and other devices.

Keywords: fullerenes, nanocrystals, high pressure, polymerization, structural transitions

PACS: 81.40.Vw, 61.48.–c, 68.37.Og, 81.30.Hd **DOI:** 10.1088/1674-1056/22/9/098109

1. Introduction

Owing to their unique structures and properties, fullerenes have attracted great attention in the studies of nanomaterials and molecule-based electronic devices.[1,2] The C_{60} molecule can be taken as a truncated icosahedron built up by all carbon atoms. There are 12 pentagons and 20 hexagons on a C_{60} cage, forming a bucky ball with all carbon atoms located at the nodes of a series of hexagons and pentagons, which is defined by alternating single and double bonds. The double bonds on the cage are highly reactive because their energies increase due to curvature induced by the cage structure. Such a curvature also results in the carbon atoms in C_{60} molecules essentially possessing sp^2 hybridized state with some contribution of the minor sp^3. As a representative zero-dimensional nano material in carbon family whose bulk modulus is twice as great as that of diamond, fullerene molecules thus become excellent building blocks for studying novel phase and constructing new carbon-based materials both under ambient pressure and high pressure conditions. Moreover, engineering unique properties are strongly dependent on the ability to control the structures, size, and morphology of the fullerene materials, which remains a crucial issue in both fullerene nanoscience and nanotechnology and their applications.

Under ambient conditions, fullerene molecules are held together by an extraordinarily weak van der Waals interaction, forming molecular crystals. Since fullerene properties depend strongly on crystals size, morphology, and structure, the fabrication of pre-designed and controllable geometries in fullerenes is critical for designing nanometer-scale electronic, optical and other devices.[3–16] Recent studies have focused on the growth of low-dimensional fullerene crystals at the nanoscale due to their superior properties.[3–15] Particular efforts have been devoted to the growth of well-dispersed fullerene nanocrystals directly on different substrates for direct applications in the filed of nanoscale devices. In the respect of fabricating well-dispersed fullerene nanocrystals, our group first developed a simple and fast evaporation method

*Project supported by the National Basic Research Program of China (Grant No. 2011CB808200), the National Natural Science Foundation of China (Grant Nos. 10979001, 11104105, 51025206, and 51032001), the Cheung Kong Scholars Programme of China, and the Changjiang Scholar and Innovative Research Team in Universities of China (Grant No. IRT1132).

†Corresponding author. E-mail: liubb@jlu.edu.cn

© 2013 Chinese Physical Society and IOP Publishing Ltd

by vaporizing the solvent from a C_{60} solution in various aromatic solvents.[7,8] In this paper, we will briefly describe recent progress made in this field.

As one of the independent thermodynamic parameters apart from those usually studied, such as temperature and composition, pressure plays an increasingly important role in physics and materials. Pressure can be effective in shortening atomic distance, enhancing orbital overlap, consequently modifying crystalline structures and tuning interactions. Thus, we can not only obtain fundamental parameters from *in situ* high pressure study, such as bulk modulus, equation of state (EOS), but also realize novel high pressure state combined with other conditions.

High pressure and high temperature serves as an efficient way of polymerizing fullerenes, creating several forms of sp^2–sp^3 C_{60} phases, such as dimers (D), one-dimensional (1D) orthorhombic (O), two-dimensional (2D) tetragonal (T) and rhombohedral (R), and three-dimensional (3D) polymeric phases.[17–19] Polymerization of C_{60} fullerene has attracted considerable attention due to the promising properties of the materials. Though the polymerization of C_{60} bulk samples has been widely studied, there have been few reports on the polymerization of C_{60} nanocrystals. For fullerene nanocrystals, one important issue is to know how the size and morphology influence the basic physical parameters compared with their corresponding bulk counterparts. On the other hand, most of the as-prepared fullerene nano/microcrystals are formed in molecular crystals with weak intermolecular interactions via either van der Waals or charge transfer, making the crystals fragile. This restricts their future applications in some fields. To build harder and stiffer forms of fullerenes, one way is to induce polymerization among the C_{60} molecules that contain C=C double bonds to create strong covalent intermolecular bonds of the sp^3 kind.[17]

Another important issue is to tune and modify the intermolecular interaction by high pressure, which plays an important role in determining the structure and properties of the fullerene crystals. In particular, in a dopant-C60s hybrid system, the presence of the intercalants strongly affects the structure of the grown crystals, as well as the electronic properties of the formed crystals via different intermolecular interactions.[8,9,20–24] Finely tuning the intermolecular interaction is thus important for tailoring the properties of fullerene crystals, which may also allow us to study the new physical process during the polymerization of fullerenes. Besides these expectations, the parameters such as nanosize effect and the special morphologies of the fullerene nano/microcrystals could also play roles in the transformations of fullerenes under pressure. Therefore, from both a fundamental and a practical point of view, high pressure studies on these fullerenes nano/microcrystals have attracted great interest.

In this review, after a brief introduction to our recent progress in controllable synthesis of fullerene nano/microcrystals by solution evaporation method developed by our group, we focus on the results of high pressure study on fullerene nano/microcrystals. The rest of this paper is organized as follows. After a general description of the progress in the growth of fullerene nano/microcrystals mostly by the fast solution evaporation method in Section 2, we present structural transformations in fullerene nano/microcrystals under pressure in Section 3. The pressure induced structural transformations and amorphization, pressure induced polymerization and novel carbon phase of long range ordered crystal with amorphous nanoclusters as building blocks in nano/microcrystals under pressure are described in this section. Finally, we give conclusions and outlook in Section 4.

2. Material preparation

The production of shape- and size-controlled fullerene crystals would enhance the utility of these molecules in tailoring their properties. Up to now, the preparation of nanometer-scale components with prescribed morphology has been achieved by different methods, including the use of templates, solution evaporation method, precipitation method, the liquid–liquid interfacial precipitation (LLIP) method, and the solvent-free vapor-driven crystallization processes.[3–14] By these methods, 1D nanorods, nanowires, nanowhiskers, nanotubes, 2D nanosheets, and 3D cubes have been produced. In particular, the direct solution vapor method is a fast and facile method to prepare fullerene single crystals on various substrates, which has always been regarded as an efficient way of fabricating fullerene crystal. Recently, we developed and extended this method to produce well dispersed 1D, 2D, and 3D nanosized fullerene single crystals (Fig. 1).[7,8,20,25,26]

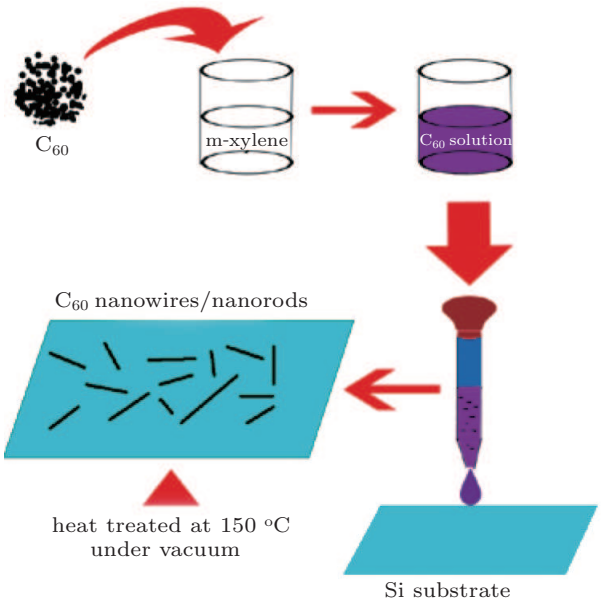


Fig. 1. Schematic drawing of the solution evaporation method of synthesizing fullerene nano/microcrystals.

By evaporating a solution of C_{60} in m-xylene, in which neat m-xylene was used as a shape controller, C_{60} can rapidly grow into thin and rectangular nanorods with widths and thicknesses on the order of nanometers.[7] The widths of the rods were in a range of 100–450 nm, and a majority of the nanorods have a width of about 200 nm; their average length was about 100 μm (Fig. 2). The diameters and length-to-diameter ratios of the synthesized nanorods can be tuned by using different growth conditions. The smallest nanorods obtained have widths smaller than 30 nm. The nanorods obtained are highly crystalline and of single phase. The as-prepared nanorods contain m-xylene solvent (C_{60}:m-xylene, 1:1) and have a hexagonal structure ($P63$ space group, $a = 2.376$ nm and $c = 1.008$ nm). The as-grown solvated nanorods exhibit a significant increase in photoluminescence (PL) intensity, which is about 2 orders of magnitude higher than that for pristine C_{60} crystals in air.[8] The interaction between C_{60} and m-xylene molecules is of the van der Waals type, which reduces the icosahedral symmetry of C_{60} molecules and induces strong PL from the solvate nanorods.

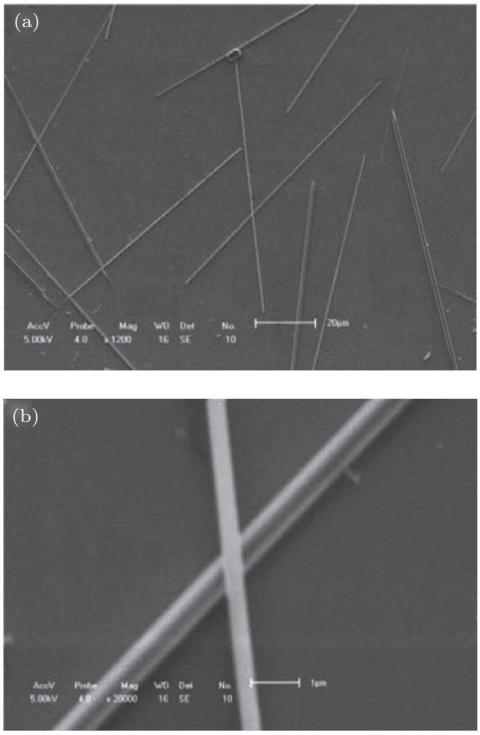


Fig. 2. Scanning electron microscope (SEM) images of C_{60} nanorods produced by evaporating C_{60}/m-xylene solution. (a) Low magnification and (b) high magnification.[27]

Moreover, the solvent can be easily removed by heating the material at above 150 °C under vacuum, which transforms the nanocrystals into FCC structure while rod shape can be preserved. It is interesting that a gradual expansion of the lattice constant is observed in the C_{60} nanorods as their widths decrease. The well-dispersed nanorods synthesized by using this method are of great benefit to their application in the field of nanoscale devices. In addition, it is interesting that 1D fullerene nanotubes can be fabricated from these as-prepared nanorods. For example, by heating the as-prepared nanorods from evaporating C_{60}/p-xylene solution at 150 °C for 10 h, the nanorods can be transformed into nanotubes. The sizes of the obtained nanotubes are dependent on the starting nanorods.

Later, the evaporation method was modified to synthesize C_{60} nanosheets on substrates, which gives no chemical reaction with the solvent and C_{60} at 150 °C.[25] The obtained C_{60} nanosheets are hexagonal crystals with lateral dimensions in the micrometer range and crystallized into an fcc structure. The average thickness of the nanosheets is about 250 nm. More interestingly, the lattice of the nanosheets is expanded by about 0.4% compared with that of bulk C_{60}. Such a lattice expansion subsequently induces the increase of the bulk modulus and stability of the C_{60} cage of the material upon compression.

To better understand the effects of solvent type on growing C_{60} nano/microcrystals by the evaporation techniques, the positional isomers, including ortho- (o-), meta- (m-) and para- (p-) type aromatic solvents have been systematically studied.[26] C_{60} crystals with various morphologies have been produced, including 1D nano/microrods and 2D sheets. C_{60} nano/microrods crystallized into a hexagonal structure have been grown on solid substrates by vaporizing solutions of C_{60} in m-type solvents. The m-dichlorobenzene gives the highest production. The diameters of the produced C_{60} rods have a wide distribution, from tens of nanometers to 5 mm. The aspect ratios of these rods could be tuned by changing the concentration of C_{60} in solution. Almost no rod-like crystals were obtained by o- and p- type solvents, but for p-type solvents some 2D or 3D nano/microcrystals with a well-crystallized fcc structure have been observed.[26] This indicates that different positional isomers have different interactions with C_{60} and therefore different abilities to shape C_{60} crystals.

The SEM image given in Fig. 3(a) directly shows that the growth of the C_{60} rods follows a nucleation-growth pathway,[26] which is a normal growth mode in some self-assembly models of molecular crystals.[28] Based on the SEM studies we also find that the smaller diameter rods grow faster than the bigger ones, making it possible for them to occasionally traverse the bigger ones during their growth. High resolution transmission electron microscopy (HRTEM) analysis shows that the hexagonal close-packed C_{60} rods grow along the (001) direction (Fig. 3(b)), which is consistent with the early reported results.[5,7]

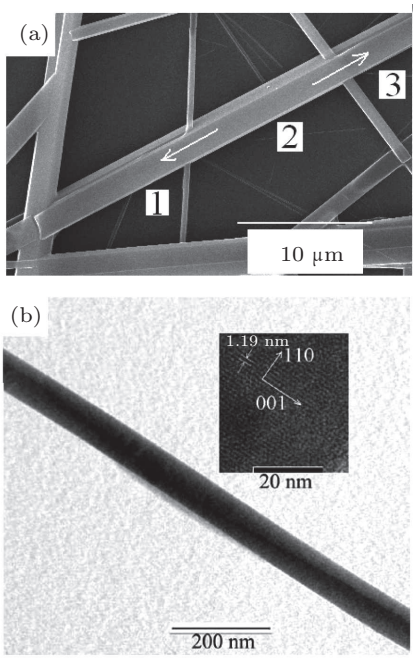


Fig. 3. (a) SEM image of the as-grown C_{60} rods, showing that rods grow along two directions, following a nucleation-growth model; and (b) HRTEM image of C_{60} rod.[26]

This series of solvents are also efficient to grow C_{70} crystals. Various C_{70} nano/microcrystals, including rods, tubes and cube shaped C_{70} microcrystals can be selectively obtained.[20] The sizes of the synthesized C_{70} cubes range from several hundreds of nanometers to tens of micrometers (> 30 μm), which could grow individually on the substrate and some also grow in an interlaced manner. Note that the m-type solvents produce microrods and/or microcrystalline cubes with either an orthorhombic or a monoclinic structure, while p-type solvents lead to cubic crystals with a hexagonal structure (possibly containing some fcc structure). In addition, the C_{70} crystals grown from m-type solvents usually contain solvent molecules while the crystals grown from p-type solvents are free from solvent. For the solvated C_{70} crystals, the interaction of solvent–C_{70} is weak van der Waals force, similar to that of solvated C_{60} crystals. Moreover, the photoluminescence (PL) efficiency of C_{70} crystals at room temperature increases with the increase in structural order, where the best crystalline C_{70} cube crystals show a 10-fold enhancement of PL efficiency compared with the polycrystalline C_{70} powder, indicating their possible implementation in optical devices.

3. Structural transformations in fullerene nano/microcrystals under pressure

3.1. High pressure induced phase transitions and amorphization

High pressure studies on nanostructured material have attracted great enthusiasm because of its many novel high pressure behaviors in the nanomaterials. Previous high pressure studies on nanomaterials have shown that the size and morphology effects have a strong influence on the critical pressure for phase transition, phase transition routine, and even amorphization process. However, high pressure studies on fullerene nanomaterials have been rarely reported. The progress in fabricating fullerene nanocrystals with designed morphologies and size has aroused significant interest in high pressure research on these nanocrytals. It is necessary to understand the size and morphology effects on the transformation of fullerenes nanocrystals under pressure.

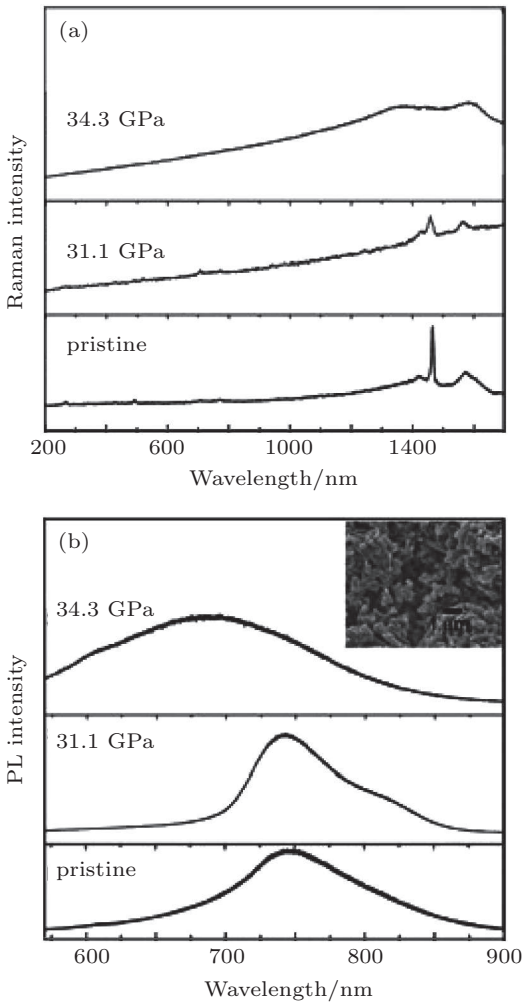


Fig. 4. Raman (a) and PL (b) spectra of C_{60} nanotubes decompressed from different pressures. Insert shows the images of C_{60} nanotubes decompressed from 31.1 GPa.[29]

C_{60} nanotube is a good model to investigate such effects on the stability of C_{60} under high pressure.[29] At the pressure between 1.46 and 2.26 GPa a phase transition from fcc to sc phase has been observed based on our *in situ* high pressure Raman measurements. However, the transition pressure is about 1 GPa higher than that observed in the bulk C_{60} crystals. *In situ* PL studies suggest that the pressure induces the stronger interaction of C_{60} molecules, which results in the decrease in the band gap of C_{60} and thus the redshift of PL bands. This change is in agreement with previous results on bulk C_{60}s. The

Raman peaks and PL spectra of the samples quenched from high pressure show that the amorphous phase reverts to the pristine crystalline C_{60} after decompression, which indicates that the C_{60} molecules are stable at 31.1 GPa in nanotubes. The C_{60} nanotubes still maintain their one-dimensional morphologies when quenched from 31 GPa (Fig. 4). However, the pressure-induced amorphization became partially irreversible when the pressure was higher than 34.3 GPa. This amorphization pressure is much higher than that for C_{60} bulk crystals reported in previous work[30] and nanosheets. The higher transition pressure and higher stability of the C_{60} cages can be ascribed to the effect of small size of nanotubes.[29] It is thus suggested that the C_{60} crystals with smaller size probably will be a good candidate for fabricating superhard materials.

In the high pressure study on C_{70} nanotubes, the small size effect on the material transformation has also been observed.[31] The C_{70} nanotubes used here were crystallized into an fcc structure with lattice constant $a = 1.492$ nm (Fig. 5), which were fabricated by a similar process to that for the synthesis of C_{60} nanotubes, followed by a heat treatment. The tubes have outer diameters in a range of 500–800 nm. Upon compression, a molecular orientation-related phase transition, from fcc structure to rhombohedral structure was observed around 1.5 GPa. Again, this transition pressure was about 1 GPa higher than that of bulk C_{70} crystals. The amorphization pressure of C_{70} nanotubes was observed at above 20 GPa and the irreversible and complete amorphization of C_{70} nanotubes was above 51.1 GPa. The pressure for this transition is much higher than that of bulk crystals. Upon decompression from 30.8 GPa, the released nanotubes partly remain their initial structures and tube-like morphologies. Decompressed from higher pressure of 43 GPa, the cage structure of C_{70} molecules is still preserved.

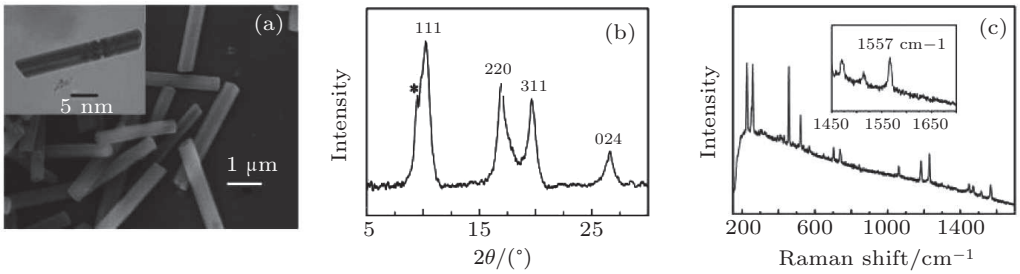


Fig. 5. (a) SEM and TEM (insert) images, (b) XRD patterns, and (c) Raman spectra for pristine C_{70} nanotubes. The fcc structure of the C_{70} tubes is the same as that of the bulk C_{70} crystal.[31]

Table 1. Amorphization pressures and bulk moduli of the studied fullerene nanocrystals.[a)]

Sample	Size	Structure	Amorphization pressure	Bulk modulus
C_{60} nanotube	$D \sim$ 300–500 nm	fcc	$>$ 34.3 GPa	26.7 ($>$ 9.8 GPa) 123.5 ($>$ 12.3 GPa)*
C_{60} nanosheet	$T \sim$ 250 nm	fcc	31 GPa	29±1.9
Bulk C_{60}	micrometers	fcc	28 GPa	15–20 GPa
C_{70} nanotube	$D \sim$ 500–800 nm	fcc	$>$ 43 GPa	50 GPa (bulk $C_{70} \sim$ 25 GPa)

[a)] D is the diameter and T is the thickness of the sample. *Results obtained from Ref. [32].

In Table 1 the amorphization pressures and the bulk moduli for the studied fullerene nanocrystals are listed and compared with those of the bulk samples. The nanosize and morphology effects are found to be important for the amorphization of fullerene nanocrystals and the increase in the high pressure stability of the fullerene cages. Moreover, the bulk moduli of the nanocrystals are obviously higher than those of the bulk. In particular, the bulk modulus of C_{70} nanotubes is about 50 GPa, which is twice larger than that of the bulk C_{70} crystal. The higher bulk modulus is due to the nanosize effect of the C_{70} nanotubes and is responsible for the higher stabilities of both the crystal structure and the molecular structure of C_{70} nanotubes.[31]

3.2. Polymerization of fullerene nanocrystals under pressure

3.2.1. Effect of charge transfer and spatial confinement on the polymerization of fullerenes under pressure

The intercalated fullerene complexes are formed by either the relatively weak van der Waals interactions or both relatively weak van der Waals interactions and charge transfer from donors to acceptors. Such interactions are expected to be modified by the application of external function such as high pressure. On the one hand, high pressure can shorten the intermolecular distance and compress the interatomic bonds, which may induce the polymerization of C_{60}s from different directions in an fcc crystal composed of free C_{60}s (Fig. 6).

It is interesting that, when the C_{60}s were confined in a 1D nanochannel of single wall carbon nanotubes, the C_{60}s can only form polymeric bonds with its two neighbors, transforming into dimer at low pressure and then 1D linear polymeric structure at high pressure.[33] This indicates that utilizing confinement environment is a possible way to realize the controllable polymerization of fullerene molecules.

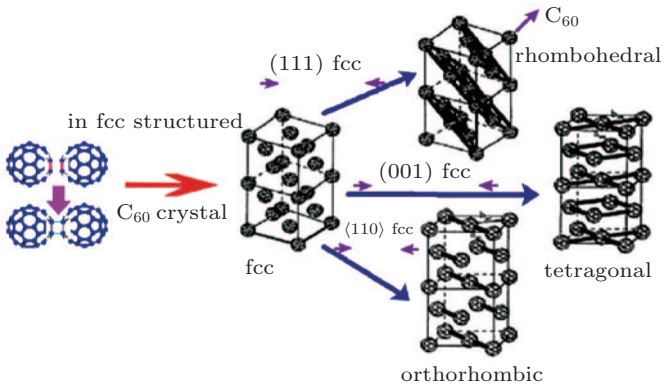


Fig. 6. Polymerization of C_{60}s and schematic map for the polymers of C_{60}s in an fcc structure.

On the other hand, the presence of dopants may modify the transformation of fullerene molecules upon compression, such as polymerization, structural deformation, and even cage collapse. Thus, compressing the intercalated fullerenes provides a possible way to create new hybrid carbon materials. Moreover, the degree of charge transfer between C_{60} molecules and dopants may be tuned by applying pressure, which is important for tuning the properties of the intercalated fullerides and thus for their potential applications. This is due to the fact that the doping can change the charge distributions, the electronic structures, and the energy gaps between the lowest unoccupied molecular orbital (LUMO) and the highest occupied molecular orbital (HOMO) of the parent fullerenes. Thus, the electronic properties of the materials may be tuned in a wide range, from insulator to superconductor.

Ferrocene (Fc, $Fe(C_5H_5)_2$) is a material which has a strong electron-donating ability but weak charger transfer to C_{60}.[34] It has been reported that the degree of charge transfer in the donor-acceptor complex is mainly determined by the vertical ionisation potentials of donors and the electron affinity of acceptors together with the efficiency of the HOMO–LUMO overlap which is related to the distance between donor and acceptor.[35] Thus, high pressure studies of Fc–C_{60} compounds provide good opportunities to study how to tune the degree of charge transfer between C_{60} and strong electron-donating dopants. The single crystalline $C_{60}(Fc)_2$ nanosheets were prepared by the procedures described in Ref. [34]. *In situ* high pressure Raman on $C_{60}(Fc)_2$ has been used to explore the pressure-induced change of charge transfer in this system and its effect on the transformation of C_{60} molecules.[36] The results

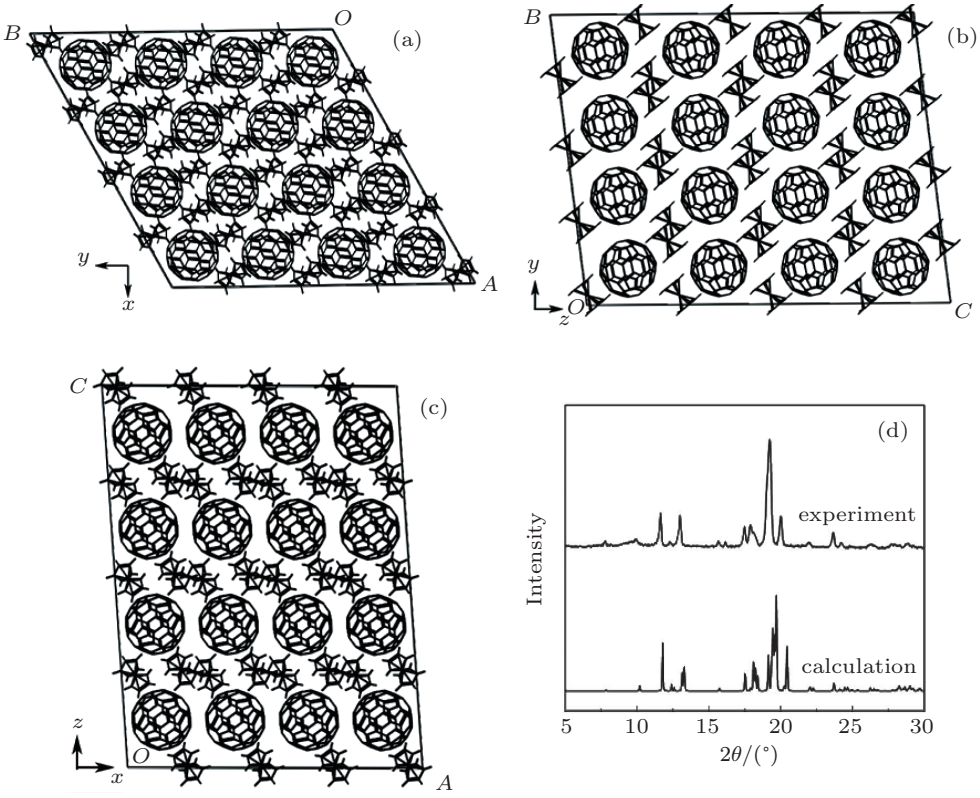


Fig. 7. Packing arrangements for $C_{60}(Fc)_2$ in the ba plane (a), bc plane (b), ca plane (c), respectively. (d) XRD pattern of $C_{60}(Fc)_2$ from experiment (top) and calculation (bottom).[36]

show that the charge transfer between Fc and C_{60} molecules can be strengthened in a low pressure range, and at above 5 GPa the C_{60} molecules start to form polymer chains. Only certain C_{60} molecules can take part in this polymerization reaction due to the special layer structure in the $C_{60}(Fc)_2$ nanosheets and the resulting spatial restriction due to the layered Fc molecules (Fig. 7). This indicates that the Fc acts not only as an electron reservoir to transfer electrons to C_{60}s and the amount of the transferred charge can be tuned by the applied pressure, but also as a spacer in the transformation of the material. The observed polymerization is found to be reversible upon decompression which is probably due to the reversibility of the pressure-tuned charge transfer interaction between Fc and C_{60} molecules. This is the first experiment showing that the polymerization of C_{60}s in doped fullerenes is affected by both charge transfer and spatial confinement, which can be tuned by the application of pressure, opening a new way of studying controllable polymerization of fullerenes.

Besides C_{60}, C_{70} is another "heavy" fullerene easily available in significant quantities and exhibits more unique and outstanding physical properties than C_{60}. However, the polymerization of C_{70} becomes less efficient due to the topochemical constraint, a specific feature of the molecule. Polymerization of C70s usually requires HPHT conditions. Motivated by the polymerization of C_{60}s in $C_{60}(Fc)_2$ hybrid assisted by charge transfer, we focused on the possible polymerization of C_{70} in $C_{70}(Fc)_2$ under pressure at room temperature. In a recent study, we used *in situ* Raman and IR spectroscopy as well as XRD to investigate the structural transitions of $C_{70}(Fc)_2$ under high pressure.[37] The synthesis process of $C_{70}(Fc)_2$is similar to that of $C_{60}(Fc)_2$ described above. Similarly, $C_{70}(Fc)_2$ was formed by weak charge transfer between the two components under ambient conditions. We find that a dimeric phase and a 1D polymer are formed above 3 and 8 GPa (Fig. 8), respectively. The polymerization is reversible when released from, at least, 20 GPa. To support our analysis we have also calculated the electron local function (ELF) and the charge transfer from $C_{70}(Fc)_2$ under pressure, from which we observed a gradual overlapping of the electron cloud around C_{70} cages, undergoing dimeric and linear polymerization (Fig. 9). The polymerization mechanisms are discussed in the framework of pressure-tuned changes in the charge transfer, the overridden steric repulsion of counterions, and the unique layered structure of $C_{70}(Fc)_2$.[37] This is the first time that we have observed a reversible pressure-tuned polymer of C_{70} doped material with the bonding between C_{70}s solely driven by the applied pressure. This material is different from those C_{70} polymers that require the combination of high pressure and high temperature treatments.

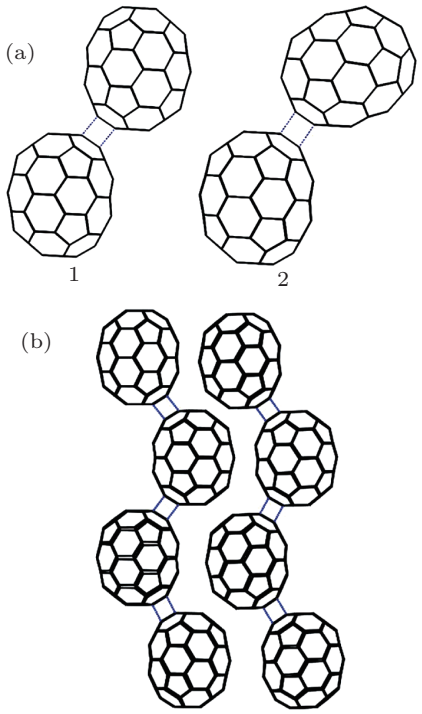


Fig. 8. Possible polymeric structures of C_{70} in C_{70}(Fc)2 crystal formed at 3.5 (a) and 8 GPa (b).[37]

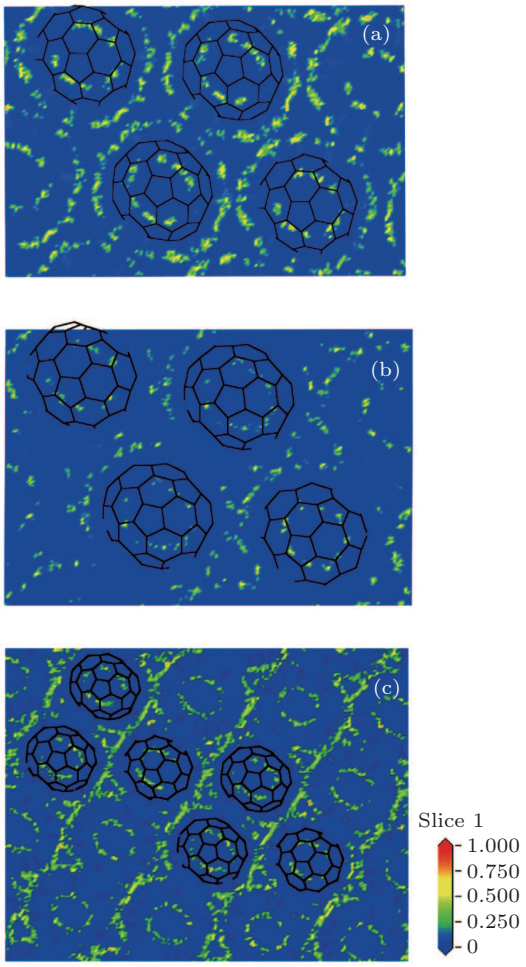


Fig. 9. ELF of the crystals viewed from the (100) plane at 2 (a), 3.5 (b), and 8 GPa (c). The green (or yellow) elliptical represents the ELF of each C_{70} molecule.[37]

3.2.2. Polymerization at high pressure and high temperature

As described above, C_{60} nanorods, nanotubes and nanosheests are all single crystals with specified growth directions. Such a morphological difference, together with the nanosize effect, may cause the different polymerization behaviors for the C_{60} nanocrystals compared with the bulk C_{60} sample. HPHT treatment has thus been carried out on the fcc structured C_{60} nanorods, nanosheets, and nanotubes (Fig. 10).[38–41] In the experiment, the C_{60} nanocrystals were located on a Mo substrate and then transferred into a big press for HPHT treatments with silicon oil as pressure medium.

C_{60} nanorods were treated under two different conditions, at 1.5 GPa and 573 K and 2 GPa and 700 K, respectively. The former condition has been used to produce orthorhombic polymeric structure in bulk C_{60}, while the latter can produce a tetragonal phase of bulk C_{60} containing minor *R* phase. The C_{60} nanorods have been transformed into similar polymeric structures when subjected to the same HPHT treatments.[38] The difference in the polymeric structures between the nanorods and the bulk is their microstructures, which will be discussed below. It is worth noting that the nanorods preserve their rod shapes after the quasi-hydrostatic pressure treatment. Owing to the nanosize effect, most of the Raman modes in polymeric nanorods are much broader than those in bulk polymeric C_{60}.

The main fluorescence band shifted from 1.697 eV (730 nm) in the unpolymerized sample to 1.657 eV (748 nm) in the *O* phase and further to near infrared 1.588 eV (780 nm) in the *T* phase. A shoulder peak at 1.74 eV in the PL spectrum of the *T* phase has also been observed. This peak has been discussed in our previous study on the *R* phase and was assumed to originate from *R* phase related surface defects.[39] The PL intensity of the polymeric samples is about ten times higher than that of pristine C_{60} nanorods in air, indicating that the polymerization greatly enhances the luminescence of C_{60} nanorods. The enhanced fluorescences with tunable frequency for different polymeric C_{60} nanorods provide a potential application in luminescent nanomaterials.

The differences in polymeric phase and PL spectrum between nanorods and bulk samples might be caused by their different morphologies. In bulk samples, a single crystal of the *O* phase contains a number of differently oriented domains after polymerization. Each domain is rather large, much greater than 20 nm and has one of 12 possible orientations relative to the original lattice because all (110) directions are equivalent for *O* phase. In the same way, the *T* phase has three equivalent directions.[42] For this reason, a disordered network structure possibly exists in the bulk polymeric samples. As for nanorod sample, the pristine C_{60} nanorod is a single crystal with specified growth directions; the (111) planes are horizontally aligned whereas the (110) planes are vertical. This probably causes relatively well-ordered domains in polymeric C_{60} nanorods compared with that in bulk polymeric samples. Such a morphological difference may cause the different PL spectra for C_{60} polymeric nanorods from those for bulk C_{60} samples.

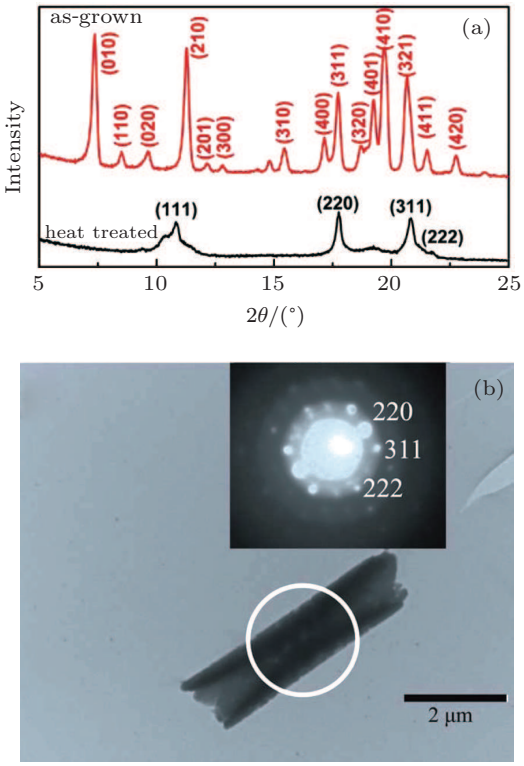


Fig. 10. (a) XRD patterns of C_{60} nanotubes obtained from solution and heat-treated at 150 °C, in vacuum. (b) TEM image and electron diffraction pattern of a selected area on a pure C_{60} nanotube.[41]

For C_{60} nanosheets after the same HPHT treatments, the produced polymeric phases are similar to those of nanorods. Their difference is that, in the HPHT-treated nanosheets at 2 GPa and 700 K, besides the *T*-phase and a trace of *R*-phase polymers, *O* phase polymer has also been observed in the sample.[40] The main fluorescence band shifted from 1.70 eV in the monomeric phase to near infrared in the polymeric phase. A comparison between PL spectra of the polymeric nanorods and those of the polymeric nanosheets from the same HPHT conditions shows only slight difference in the relative intensity of the PL peaks in the polymeric nanosheets which can be observed. The differences in PL and Raman spectra between nanosheets and nanorods samples treated under the same conditions are probably caused by different polymerization degrees in these samples because of different shapes.[40]

Now we turn to the results on C_{60} nanotubes with the same HPHT treatments. The fcc structured C_{60} nanotubes ($a = 1.415$ nm) used here have diameters ranging from 300 to 500 nm and hexagonal cross-sections (Fig. 10). The selected area electron diffraction (SAED) pattern indicates that the longitudinal direction of the tubes is along the [110] orientation. The morphology of the nanotubes can be retained

after the HPHT treatments (Fig. 11). Treating the nanotubes at 1.5 GPa and 573 K results in a dimeric polymer phase of the sample, while linear polymeric structure (orthorhombic phase) has been observed as dominant phase in the nanotubes sample after the treatment at 2 GPa and 700 K.[41] These polymeric structures of nanotubes show low polymer degree compared with those of the bulk crystals treated at same HPHT conditions. The results indicate that C_{60} nanotubes are more difficult to be polymerized than the bulk single crystals, which has been explained by the fact that the molecule packing and small hollow structure of nanotubes give large constraints to the development of long-range-ordered polymers. In addition, PL measurements show that the PL positions of HPHT treated nanotubes are blue-shifted with the increase of the applied pressure and temperature. A detailed comparison in the polymeric phases and PL among the C_{60} nanorods, nanosheets, nanotubes and the bulk crystals is listed in Table 2. The morphology-dependent polymerization of C_{60} nanocrystal can be clearly observed. It is interesting that the polymerization of fullerene molecules strongly affects the PL of the nanotube samples but this tendency of the PL behavior is not obvious for the bulk crystals. This indicates that it is possible to tune the optical properties of the nanotubes by applying a pressure.

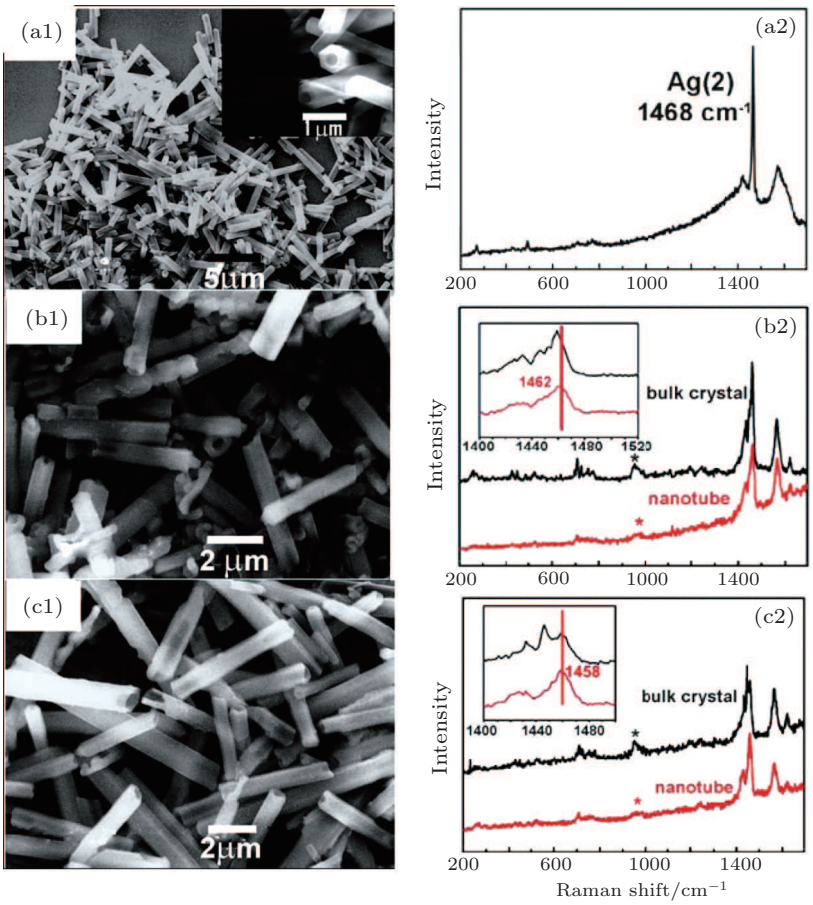


Fig. 11. SEM images (Left) and corresponding Raman spectra (Right) of (a) pristine C_{60} nanotubes, and of C_{60} nanotubes after treatment at (b) 1.5 GPa, 573 K and (c) 2 GPa, 700 K.[41]

Table 2. PL peaks of C_{60} bulk crystals and nanocrystals treated under different pressures and temperatures, and the assignment of these peaks. The peaks marked with * are the strongest peaks for each sample.

	Bulk crystals		Nanotubes		Nanosheets		Nanorods	
Treatment conditions	Energy	Phase	Energy	Phase	Energy	Phase	Energy	Phase
1.5 GPa, 573 K	1.53 eV	*R*	1.53 eV	*R*	1.53 eV	*R*	1.53 eV	*R*
	1.66 eV(*)	*O*	1.66 eV(*)	*D*	1.66 eV(*)	*O*	1.66 eV(*)	*O*
	1.74 eV	–			1.74 eV	–	1.74 eV	–
2.0 GPa, 700 K	1.45 eV	*T*						
	1.53 eV	*R*						
	1.58 eV	*T*	1.60 eV(*)	*O*	1.53 eV	*R*	1.53 eV	*R*
	1.68 eV	*O*	1.65 eV(*)	*O*	1.58 eV(*)	*T*	1.58 eV(*)	*T*
	1.74 eV(*)	–	1.74 eV	–	1.74 eV	–	1.74 eV	–

To further understand the difference in C_{60} polymerization between the nanocrystals and the bulk, we take the nanotubes as an example. A model of a single nanotube is shown in Fig. 12. From the top moiety it is shown that except for the [110] growth direction all the other [110] directions are either perpendicular to or have an angle of $\pi/3$ with respect to the axis of nanotube, indicating that the linear extent of lattice in the [111] directions is limited to the range of nanometres. C_{60} nanotubes have even smaller dimensions in these directions due to their hollow structure. For the bulk C_{60}s, there are 12 possible equivalent [110] orientations in the fcc lattice for the *O* phase and *T* phase may form in all the [110] orientations in the three equivalent (001) planes. The molecular packing is confined on the nanoscale and lacks long-range order, so all these orientations are not available for polymerization on the nanocrystals and nanomaterials often exhibit higher phase transformation pressures. Therefore, the polymerization in these directions that have nanoscale dimensions requires higher pressure than in the growth directions.

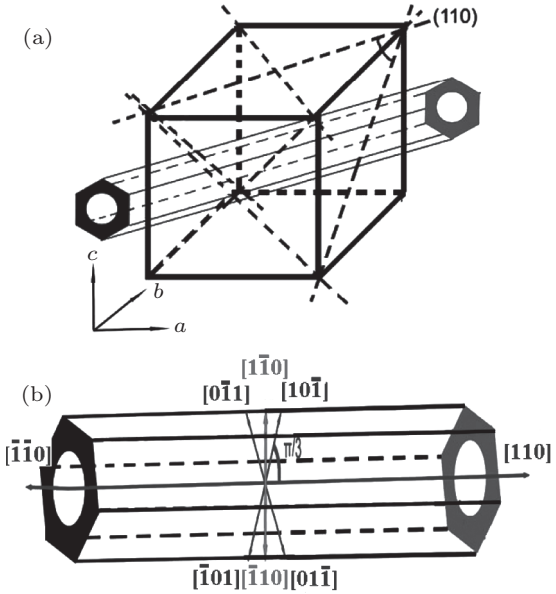


Fig. 12. (a) Model of a single nanotube in the frame of the fcc structure, which shows that the nanotube grows along the [110] direction, (b) top view of this single tube, showing all the [110] direction in the tubes viewed from the top in panel (a).[41]

3.3. Novel carbon phase from compressing solvated C_{60} crystals

From the above high pressure studies at ambient temperature we learn that when the solvent has been removed from the as-prepared crystals and the dopant–C_{60} interaction is absent, the fullerene molecules on the nanocrystals face to each other and their high pressure behaviors are similar to those of the bulk pure fullerene crystals. The small size and the quasi-1D morphology effects play dominant roles in the critical transformation pressures of the materials under pressure. By contrast, when the solvent is preserved in the crystal lattice, the transformation of the material is affected by both the interaction of dopant-fullerene molecules and the spatial constraint of the solvent in some directions. In a fullerene hybrid constructed by aromatic solvents and fullerenes via weak van der Waals, such a spatial confinement effect from the solvent should play a dominant role in the pressure-induced transformations.

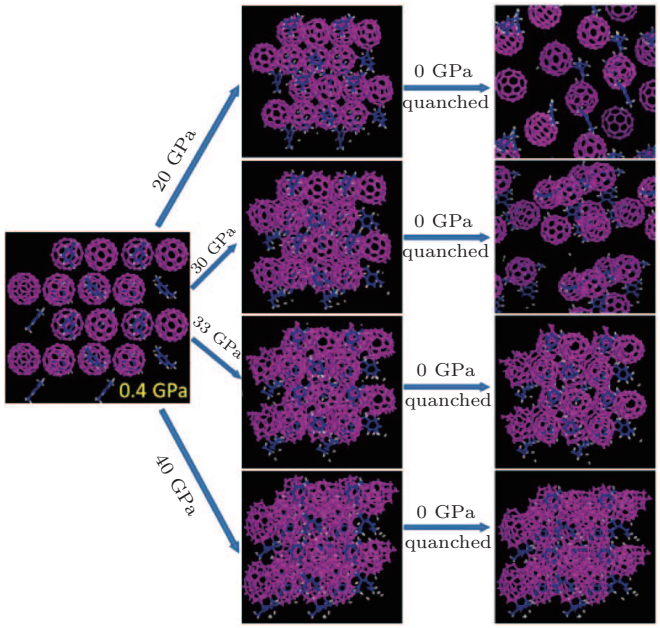


Fig. 13. Simulated structures of the material under different compression and decompression conditions. The deformation of the C_{60} cages is elastic below approximately 30 GPa, and the deformed cages return to their initial shape as they are decompressed back to ambient pressure. At above 30 GPa, many carbon-carbon bonds start to break, and the cages can no longer return back to C_{60} upon decompression. OACC maintains long-range periodicity, and can be preserved under ambient pressure conditions.[43]

Very recently, Wang *et al.*[43] compressed solvated C_{60}s (C_{60}*m-xylene) at room temperature and obtained a novel carbon phase that is called ordered amorphous carbon clusters (OACC). In this study, Raman spectra on decompressed samples show that C_{60} molecules from the crystalline solvated fullerene phase undergo an order-to-disorder transition under compression at ∼35 GPa, i.e., C_{60} cage collapses into amorphous carbon clusters. However, the X-ray diffraction reflections typical of a hexagonal close-packed (hcp) lattice and the broad oscillations of diffuse scattering typical of amorphous materials still can be observed in the material, suggesting that the amorphous carbon clusters keep their translational symmetry. This suggests that a material can still possess long-range order even though its fundamental building blocks are disordered. Such a novel phase formed has not been observed before and breaks the categorization of traditional solid state materials. The transformation of the materials has been further demonstrated by their quantum molecular dynamics (QMD) simulations. In the simulation, a similar close-packing (face-centered cubic) system was used as a test model system (Fig. 13). Below ∼30 GPa, the deformation is elastic. However, above 30 GPa, the deformation becomes so large

that a phase transition is triggered, and C_{60} molecules start to collapse by breaking the sp^2 hybrid C–C double bonds and forming new sp^3 hybrid C–C bonds. The transformation becomes irreversible upon decompression. At even higher pressures (>35 GPa), the C_{60} cages completely collapse and transform into highly disordered carbon clusters forming OACC; OACC maintains the long-range periodicity due to the presence of the solvent molecules and can be preserved back to ambient pressure conditions. The simulation results are consistent with their experimental observations. Moreover, the proposed OACC phase exhibits very high hardness and can indent diamond anvils at high pressure.

It is generally accepted that the solvent plays an important role in forming the OACC phase, but how the solvent works is not well understood. To clarify the roles of the solvents in transforming the C_{60} molecules, we recently performed comparative experiments on solvated and desolvated C_{60} crystals under pressure by *in situ* Raman spectroscopy.[44] The results show that the pressure-induced bonding change, structural transformations of C_{60}s in the two materials are quite similar, both undergoing deformation and amorphization. Nevertheless, the two materials behave differently at high pressure: the high pressure phases of solvated C_{60} can indent diamond anvil while that of desolvated C_{60}s can not. This indicates that the microstructures of their high pressure phases are probably different. Further TEM observations show that the quenched phase contains ordered phases and disordered phases (Fig. 14(a)), while Raman spectrum studies and laser irradiation on the decompressed samples revealed the amorphous nature of the composed building blocks (see Fig. 14(b) and Refs. [45] and [46]). This suggests that most C_{60}s are collapsed but still a fraction of them may preserve the periodic arrangement. Concerning the high pressure phase, the inelastic X-ray scattering (IXS) from Ref. [43] revealed a complete transition from sp^2 carbon (that of native C_{60}) to sp^3 carbon in the material at pressure above 36 GPa. Note that in the solvated sample about 10% of sp^2 carbons are from the π-aromatic rings of m-xylene. This part should also transform into sp^3 carbons by covalent bonding with highly compressed or collapsed C_{60}, which is reasonable since π-aromatic rings of the solvent are similar to those on C_{60} cage and the bonding of these π-aromatic rings is possible. In addition, our Raman data on the released sample from 20.5 GPa show that the polymerization of C_{60}s takes place, suggesting that C_{60} molecules can polymerize with neighbors at high pressure. We thus conclude that m-xylene acts as a bridge and also as a spacer to stabilize the periodic structure of the high pressure phase and the high pressure phase is a polymeric phase composed of amorphized C_{60}s and a small number of intact C_{60}s, which are kept in position by the solvent molecules in the lattice. Such polymeric carbons formed 3D network is superhard.

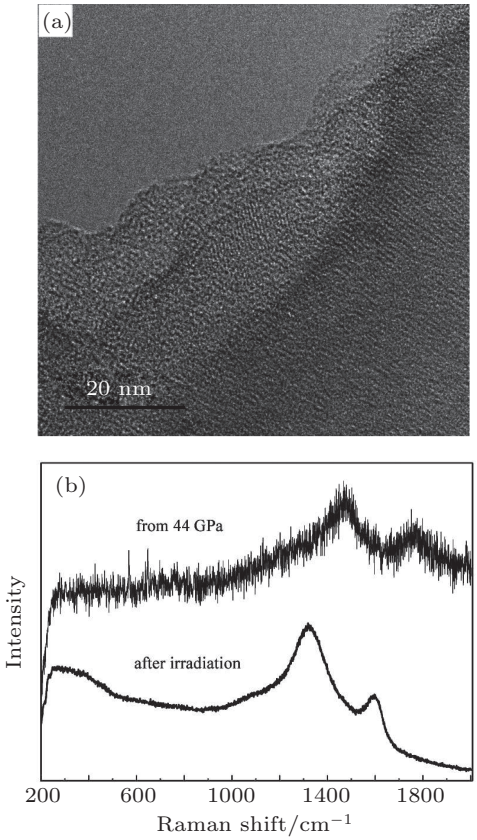


Fig. 14. (a) HRTEM image of the solvated C_{60}s sample released from 44GPa; (b) Raman spectra from the solvated sample from 44 GPa and after laser irradiation. The spectrum suggests that the released amorphous fullerene phase from 44 GPa is depolymerized into sp^2 carbon rich amorphous carbon clusters.

4. Conclusion and outlook

By using the facile solvent-assisted evaporation method, 1D fullerene nanorods, nanotubes, 2D nanosheets, and 3D cubes can be selectively synthesized by selecting suitable solvents as shape controller. Solvents play critical roles in shaping the fullerene crystal morphologies and tuning their crystal structure and properties.

C_{60} nanocrystals, including rods, sheets and tubes have been polymerized by HPHT. The polymerization of fullerenes is affected by the special morphologies of the nanocrystals, which influences the optical properties of the polymeric nanocrystals. Single-crystalline nanorods show advantages in the formation of polymerized structure compared with the bulk due to the special morphology. Furthermore, we show that high pressure serves as an efficient technique for tuning the intermolecular interaction and the amount of the charge transfer and thus the polymerization of fullerene molecules, thereby paving the way for the creation of new carbon-based materials. When the solvent is removed from the as-grown nano/microcrystals, the high pressure induced transformation sequence of fullerene crystals is similar to that of the bulk counterparts, while the nanosize effect and the special crystal geometries of the nanocrystals play dominant roles in the transformation pressure. The nanocrystals exhibit higher bulk

modulus and higher pressure stability when subjected to compression, which is explained by their nanosized dimension and slight lattice expansion. The changes of the pressure-tuned optical property in the 1D nanotubes are observed. Moreover, compressing solvated fullerene crystals induces the collapse and amorphization of C_{60} cages while the solvent is still preserved, creating a new carbon phase, in which the amorphized carbon clusters are still arranged into a long-range periodic structure. The high pressure phase of this structure is a polymeric phase composed of amorphized fullerene and a small number of intact C_{60}s, which are kept in position by the solvent molecules in the lattice. Such polymeric carbons formed 3D network is superhard and can indent diamond anvil at high pressure. It will be interesting to perform further study to understand the band structure of such a crystalline material composed of amorphous building blocks, which may bring new insight into this type of new hybrid hard materials.

We thus show here the progress in making new fullerene-based materials with fullerene molecules as building blocks, paving the way for producing new carbon materials with novel structure and properties for various application.

References

[1] Briseno A L, Mannsfeld S C B, Ling M M, Liu S, Tseng R J, Reese C, Roberts M E, Yang Y, Wudl F and Bao Z 2006 *Nature* **444** 913

[2] Dresselhaus M S, Dresselhaus G and Eklund P C 1996 Science of Fullerenes and Carbon Nanotubes (San Diego: Academic Press)

[3] Liu H B, Li Y L, Jiang L, Luo H Y, Xiao S Q, Fang H J, Li H M, Zhu D B, Yu D P, Xu J and Xiang B 2002 *J. Am. Chem. Soc.* **124** 13370

[4] Miyazawa K, Kuwasaki Y, Obayashi A and Kuwabara K 2002 *J. Mater. Res.* **17** 83

[5] Minato J and Miyazawa K 2005 *Carbon* **43** 2837

[6] Jin Y, Curry R J, Sloan J, Hatton R A, Chong L C, Blanchard N, Stolojan V, Kroto H W and Silva S R P 2006 *J. Mater. Chem.* **16** 3715

[7] Wang L, Liu B B, Liu D D, Yao M G, Hou Y Y, Yu S D, Cui T, Li D M, Zou G T, Iwasiewicz A and Sundqvist B 2006 *Adv. Mater.* **18** 1883

[8] Wang L, Liu B B, Yu S D, Yao M G, Liu D D, Hou Y Y, Cui T and Zou G T 2006 *Chem. Mater.* **18** 4190

[9] Geng J F, Zhou W Z, Skelton P, Yue W B, Kinloch I A, Windle A H and Johnson B F G 2008 *J. Am. Chem. Soc.* **130** 2527

[10] Sathish M and Miyazawa K 2007 *J. Am. Chem. Soc.* **129** 13816

[11] Sathish M, Miyazawa K and Sasaki T 2007 *Chem. Mater.* **19** 2398

[12] Ji H X, Hu J S, Wan L J, Tang Q X and Hu W P 2008 *J. Mater. Chem.* **18** 328

[13] Larsen C, Barzegar H R, Nitze F, Wågberg T and Edman L 2012 *Nanotechnology* **23** 344015

[14] Shin H S, Yoon S M, Tang Q, Chon B, Joo T and Choi H C 2008 *Angew. Chem. Int. Ed.* **47** 693

[15] Lu G H, Li L G and Yang X N 2008 *Small* **4** 601

[16] Céolin R, Tamarit J L, López D O, Barrio M, Agafonov V, Allouchi H, Moussa F and Szwarc H 1999 *Chem. Phys. Lett.* **314** 21

[17] Sundqvist B 1999 *Adv. Phys.* **48** 1

[18] Yamanaka S, Kubo A, Inumaru K, Komaguchi K, Kini N S, Inoue T and Irifune T 2006 *Phys. Rev. Lett.* **96** 76602

[19] Yao M G, Pischedda V, Mezouar M, Sundqvist B, Wågberg T, Debord R and San Miguel A 2011 *Phys. Rev B* **84** 144106

[20] Yao M G, Fan X H, Liu D D, Liu B B and Wågberg T 2012 *Carbon* **50** 209

[21] Ganin A Y, Takabayashi Y, Khimyak Y Z, Margadonna S, Tamai A, Rosseinsky M J, Prassides K 2008 *Nat. Mater* **7** 367

[22] Wakahara T, D'Angelo P, Miyazawa K, Nemoto Y, Ito O, Tanigaki N, Bradley D D C and Anthopoulos T D 2012 *J. Am. Chem. Soc.* **134** 7204

[23] Takeya H, Kato R, Wakahara T, Miyazawa K, Yamaguchi T, Ozaki T, Okazaki H and Takano Y 2013 *Mater. Res. Bull.* **48** 343

[24] Cui W, Liu D D, Yao M G, Li Q J, Liu R, Liu Z D, Wu W, Zou B, Cui T, Liu B B and Sundqvist B 2011 *Diam. Relat. Mater.* **20** 93

[25] Wang L, Liu B B, Liu D D, Yao M G, Yu S D, Hou Y Y, Zou B, Cui T, Zou G T, Sundqvist B, Luo Z G, Li H, Li Y C, Liu J, Chen S J, Wang G R and Liu Y C 2007 *Appl. Phys. Lett.* **91** 103112

[26] Yao M G, Andersson B M, Stenmark P, Sundqvist B, Liu B B and Wågberg T 2009 *Carbon* **47** 1181

[27] Wang L 2006 *Fabrication of Nano-crystals of Fullerenes with Different Shapes and Investigations of Their Physical Properties and High Pressure Induced Phase Transition* (Ph.D dissertation) (Changchun: Jilin University) (in Chinese)

[28] Jonkheijm P, van der Schoot P, Schenning A P H J and Meijer E W 2006 *Science* **313** 80

[29] Liu D D, Yao M G, Li Q J, Cui W, Wang L, Li Z P, Liu B, Lü H, Zou B, Cui T, Liu B B and Sundqvist B 2012 *J. Raman Spectrosc.* **43** 737

[30] Yoo C S and Nellis W J 1992 *Chem. Phys. Lett.* **198** 379

[31] Liu D D, Yao M G, Wang L, Li Q J, Cui W, Liu B, Liu R, Zou B, Cui T, Liu B B, Liu J, Sundqvist B and Wågberg T 2011 *J. Phys. Chem. C* **115** 8918

[32] Hu J Y, Liang S C, Piao G Z, Zhang S J, Zhang Q H, Yang Y, Zhao Q, Zhu K, Liu Y L, Tang L Y, Li Y C, Liu J, Jin C Q and Yu R C 2011 *J. Appl. Phys.* **110** 014301

[33] Zou Y G, Liu B B, Wang L C, Liu D D, Yu S D, Wang P, Wang T Y, Yao M G, Li Q J, Zou B, Cui T, Zou G T, Wågberg T, Sundqvist B and Mao H K 2009 *Proc. Natl. Acad. Sci. USA* **106** 22135

[34] Wakahara T, Sathish M, Miyazawa K, Hu C P, Tateyama Y, Nemoto Y, Sasaki T and Ito O 2009 *J. Am. Chem. Soc.* **131** 9940

[35] Konarev D V, Lyubovskaya R N, Drichko N V, Yudanva E I, Shul'ga Y M, Litvinov A L, Semkin V N and Tarasov B P 2000 *J. Mater. Chem.* **10** 803

[36] Cui W, Yao M G, Liu D D, Li Q J, Liu R, Zou B, Cui T and Liu B B 2012 *J. Phys. Chem. B* **116** 2643

[37] Cui W, Yao M G, Yao Z, Ma F X, Li Q J, Liu R, Liu B, Zou B, Cui T, Liu B B and Sundqvist B 2013 *Carbon* **62** 447

[38] Hou Y Y, Liu B B, Wang L, Yu S D, Yao M G, Chen A, Liu D D, Cui T, Zou G T, Iwasiewicz A and Sundqvist B 2006 *Appl. Phys. Lett.* **89** 181925

[39] Hou Y Y, Liu B B, Ma H A, Wang L, Zhao Q, Cui T, Hu Q, Chen A, Liu D D, Yu S D, Jia X P, Zou G T and Sundqvist B 2006 *Chem. Phys. Lett.* **423** 215

[40] Liu B B, Hou Y Y, Wang L, Liu D D, Yu S D, Zou B, Cui T, Zou G T, Iwasiewicz-Wabnig A and Sundqvist B 2008 *Diam. Relat. Mater.* **17** 620

[41] Liu D D, Yao M G, Li Q J, Cui W, Zou B, Cui T, Liu B B, Sundqvist B and Wågberg T 2011 *Crystengcomm* **13** 3600

[42] Sundqvist B 2004 *Struct. Bonding (Berlin)* **109** 85

[43] Wang L, Liu B B, Li H, Yang W G, Ding Y, Sinogeikin S V, Meng Y, Liu Z X, Zeng X C and Mao W L 2012 *Science* **337** 825

[44] Yao M G, Cui W, Xiao J P, Chen S L, Cui J X, Liu R, Cui T, Zou B, Liu B B and Sundqvist B 2013 *Appl. Phys. Lett.* **103** 071913

[45] Ferrari A C 2007 *Solid State Commun.* **143** 47

[46] Sato K, Saito R, Oyama Y, Jiang J, Cancado L, Pimenta M, Jorio A, Samsonidze G G, Dresselhaus G and Dresselhaus M S 2006 *Chem. Phys. Lett.* **427** 117